European Review for Medical and Pharmacological Sciences 2019; 23: 3042-3050

Effect of IL-6-mediated STAT3 signaling pathway on myocardial apoptosis in mice with dilated cardiomyopathy

Q. LI[1], W.-X. YE[1], Z.-J. HUANG[1], Q. ZHANG[1], Y.-F. HE[2]

[1]Department of Geriatrics, Quanzhou First Hospital of Fujian Medical University, Quanzhou, China
[2]Department of Ultrasound, Wuhan Asia Heart Hospital, Wuhan, China

Abstract. – OBJECTIVE: To investigate the effect of interleukin-6 (IL-6) gene knockout on apoptosis of myocardial cells in mice with Coxsackievirus B3 (CVB3)-induced dilated cardiomyopathy (DCM) and its potential mechanism, so as to provide certain references for the clinical prevention and treatment of DCM.

MATERIALS AND METHODS: A total of 40 male C57 mice were randomly divided into Sham group (n=20) and DCM group (n=20) using a random number table. Another 20 mice with IL-6 gene knockout were enrolled into DCM+IL-6 KO group (n=20). The DCM model was established via CVB3 repeated incremental infection. After 9 months, the heart weight/body weight (HW/BW) ratio of mice in each group was detected. The ejection fraction [EF (%)] and fraction shortening [FS (%)] of mice in each group were detected via two-dimensional ultrasonography. The cross-sectional area and pathological changes in myocardial cells in the heart in each group were determined using hematoxylin-eosin (HE) staining. The collagen content in myocardial tissues in each group was detected via Masson staining and picrosirius red (PSR) staining, and the expressions of Collagen I and Collagen III in myocardial tissues in each group were detected via immunohistochemistry. In addition, the myocardial apoptosis in myocardial tissues in each group was detected via terminal deoxynucleotidyl transferase-mediated dUTP nick end labeling (TUNEL) staining. Finally, the protein expression levels of B-cell lymphoma-2 (Bcl-2), Bcl-2 associated X protein (Bax), phosphorylated signal transducer and activator of transcription 3 (p-STAT3), and total STAT3 (t-STAT3) were detected via Western blotting.

RESULTS: The expression of IL-6 messenger ribonucleic acids (mRNAs) in myocardial tissues in DCM group was significantly increased compared with that in Sham group ($p<0.05$). After IL-6 knockout, the HW/BW ratio of DCM mice significantly declined ($p<0.05$), and the cross-sectional area of myocardial cells was significantly reduced ($p<0.05$). According to the results of echocardiography, the cardiac function of mice in DCM+IL-6 KO group was significantly superior to that in DCM group, manifested as the significant increase in FS (%) and EF (%) ($p<0.05$). The results of Masson staining, PSR staining, and immunohistochemical staining showed that IL-6 knockout could reduce the collagen content and Collagen I and Collagen III expressions in myocardial tissues of DCM mice ($p<0.05$). Furthermore, it was found via TUNEL staining that the number of apoptotic myocardial cells in DCM+IL-6 KO group was markedly smaller than that in DCM group ($p<0.05$). At the same time, the Bax/Bcl-2 ratio in myocardial tissues in DCM+IL-6 KO group was lower ($p<0.05$). Finally, the results of Western blotting revealed that DCM+IL-6 KO group had a lower phosphorylation level of STAT3 than DCM group ($p<0.05$).

CONCLUSIONS: Inhibiting IL-6 gene may improve the DCM-induced myocardial remodeling through reducing myocardial apoptosis.

Key Words:
Dilated cardiomyopathy, Myocardial fibrosis, Myocardial apoptosis, IL-6.

Introduction

Cardiomyopathy is mainly characterized by abnormalities in the ventricular size, ventricular wall thickness and systolic function, and it is manifested as the systolic or diastolic dysfunction without coronary artery disease, hypertension, valvular disease or congenital heart disease, which is divided into primary and secondary cardiomyopathy[1,2]. Dilated cardiomyopathy (DCM) is the most common cardiomyopathy in the world, and it has many causes, manifested as the impairment of systolic and diastolic function of the left ventricle or double ventricles[3]. The causes of primary DCM mainly include familial inheritance and

Corresponding Author: Yafeng He, MM; email: drheyafeng@foxmail.com

infectious factors, while the causes of secondary DCM include poisoning, autoimmune diseases, and perinatal period[4]. The pathogenesis of DCM is complex and involves the abnormal expression of multiple genes or proteins. Currently, the pathogenesis of DCM remains unclear yet[5]. Therefore, further exploring the molecular biological mechanism of DCM occurrence and development is of great significance in the early prevention and precise treatment of DCM.

Interleukin-6 (IL-6) is a classical pro-inflammatory cytokine with a very strong ability to activate the inflammation[6]. In animal models, the serum IL-6 level in mice is significantly increased at 6 h after myocardial ischemia/reperfusion[7]. IL-6 can promote the synthesis and release of pro-inflammatory mediators in various cell types. In patients with acute myocardial infarction, the serum IL-6 level is closely associated with the development of heart failure within 24 h after angioplasty[8]. IL-6 and IL-1 can synergize with tumor necrosis factor-α (TNF-α) to damage the contraction function of myocardial cells in burned mice[9]. The above results indicate that IL-6 may play a crucial role in cardiomyopathy. However, the role of IL-6 in DCM-induced myocardial remodeling and its mechanism have not been reported yet.

In the present study, the gene knockout mice were selected to establish the DCM model; the effects of IL-6 knockout on cardiac function, cardiac hypertrophy, and myocardial fibrosis in DCM mice were detected, and the potential molecular mechanism of IL-6 knockout in myocardial damage was analyzed.

Materials and Methods

Animal Grouping and Treatment

A total of 40 male C57 mice aged 8-10 weeks old weighing (24.61±1.64) g were divided into Sham group (n=20) and DCM group (n=20) using a random number table. Another 20 mice with IL-6 gene knockout were enrolled into DCM+IL-6 KO group (n=20). There were no statistically significant differences in such basic data as week age and body weight among the three groups. The DCM model was established as follows: in DCM group and DCM+IL-6 KO group, 0.1 mL Coxsackievirus B_3 (CVB_3) (10^{-5} TCD_{50}) dissolved in Eagle's Minimum Essential Medium (EMEM) was intraperitoneally inoculated and dissolved into mice, and the virus load was increased by 0.05 mL every month for a total of 9 times. After 9 months, the mice were executed, the myocardial tissues were taken from the left ventricular anterior wall, and the blood residue was washed away with normal saline. The tissues were stored in a refrigerator at -80°C for later use. This investigation was approved by the Animal Ethics Committee of Fujian Medical University Animal Center.

Detection of IL-6 Expression in Myocardial Tissues Via Reverse Transcription-Polymerase Chain Reaction (RT-PCR)

(1) The total RNA was extracted from myocardial tissues using the TRIzol method (Invitrogen, Carlsbad, CA, USA), the concentration and purity of RNA extracted were detected using an ultraviolet spectrophotometer, and the RNA with absorbance $(A)_{260}/A_{280}$ of 1.8-2.0 could be used. (2) The messenger RNA (mRNA) was synthesized into the complementary deoxyribonucleic acid (cDNA) through RT and stored in the refrigerator at -80°C. (3) RT-PCR system: 2.5 μL 10× Buffer, 2 μL cDNAs, 0.25 μL forward primers (20 μmol/L), 0.25 μL reverse primers (20 μmol/L), 0.5 μL dNTPs (10 mmol/L), 0.5 μL Taq enzymes (2×10^6 U/L), and 19 μL ddH_2O. The amplification system of RT-PCR was the same as above.

Hematoxylin-Eosin (HE) Staining

The myocardial tissues obtained in each group were placed in 10% formalin overnight, and then dehydrated and embedded in paraffin. Then, all myocardial tissues were sliced into 5 μm-thick sections, fixed on a glass slide and baked dry, followed by staining. According to the instructions, the sections were soaked in xylene, ethanol in gradient concentration and hematoxylin, respectively, and sealed with resin. After drying, the sections were observed and photographed under a light microscope to observe the morphology of myocardial cells, cardiac stroma, and myofilament.

Masson Staining

First, the paraffin sections were deparaffinized and chromized or the mercury salt precipitate was removed. Then, the sections were washed with tap water and distilled water, and the nucleus was stained with Regaud's or Weigert's hematoxylin for 5-10 min. After the sections were fully washed, they were stained with Masson Ponceaux acid fuchsin for 5-10 min. Then, the sections were immersed in 2% glacial acetic acid aqueous solution for a while, and differentiated with 1% phos-

phomolybdic acid aqueous solution for 3-5 min. Finally, the sections were transparentized with 95% alcohol, anhydrous alcohol and xylene, and sealed with neutral balsam.

Echocardiography

To detect the cardiac function of mice in each group, echocardiography was performed using the Mylab 30CV ultrasound system (Esaote SPA, Genoa, Italy) and 10-MHz linear ultrasound transducer. After the pre thoracic hair was shaved off and the mice were anesthetized, they were placed on a heating plate at 37°C with the left side upward. Then, the ejection fraction [EF (%)], fraction shortening [FS (%)], and beats per minute (BPM) were detected.

Immunohistochemical Staining

The myocardial tissue sections were baked in an oven at 60°C for 30 min, deparaffinized with xylene (5 min × 3 times), and dehydrated with 100% ethanol, 95% ethanol, and 70% ethanol for 3 times. Then, the endogenous peroxidase activity was inhibited with hydrogen peroxide-methanol at a concentration of 3%. The tissues were sealed with goat serum for 1 h, incubated with the anti-tumor necrosis factor-α (TNF-α) antibody (diluted at 1:200 with PBS) at 4°C overnight, and washed with phosphate-buffered saline (PBS) for 4 times on a shaker. Then, the secondary antibody was added, and the color was developed using diaminobenzidine. After that, 6 samples were randomly selected in each group and 5 fields of view were randomly selected in each sample, followed by photography under an optical microscope (200× and 400×).

Western Blotting Detection

The myocardial tissues of mice in each group were fully ground in the lysis buffer, followed by ultrasonic lysis. Then, the lysis buffer was centrifuged, and the supernatant was taken and placed into the Eppendorf (EP) tube. The protein concentration was detected *via* ultraviolet spectrometry, and the concentration of the protein samples was quantified to be the same. The protein was sub-packaged and placed in the refrigerator at -80°C. After the total protein was extracted, Sodium Dodecyl Sulfate-Polyacrylamide Gel Electrophoresis (SDS-PAGE) was performed. Then, the protein in the gel was transferred onto a polyvinylidene difluoride (PVDF) membrane (Millipore, Billerica, MA, USA), incubated with the primary antibody at 4°C overnight and then incubated again with the goat anti-rabbit secondary antibody in a dark place for 1 h. The protein band was scanned and quantified using the Odyssey scanner, and the level of protein to be detected was corrected using glyceraldehyde-3-phosphate dehydrogenase (GAPDH).

Statistical Analysis

Statistical Product and Service Solutions (SPSS) 22.0 software (IBM, Armonk, NY, USA) was used for the analysis of all data. Measurement data were expressed as mean ± standard deviation, and *t*-test was used for the comparison of data between the two groups. $p<0.05$ suggested that the difference was statistically significant.

Results

Expression of IL-6 In Myocardial Tissues in DCM Mice

The expression level of IL-6 mRNAs in myocardial tissues in Sham group, DCM group, and DCM+IL-6 KO group was detected. The results revealed that the expression level of IL-6 mRNAs in myocardial tissues was significantly increased in DCM group ($p<0.05$), while it significantly declined in DCM+IL-6 KO group (Figure 1).

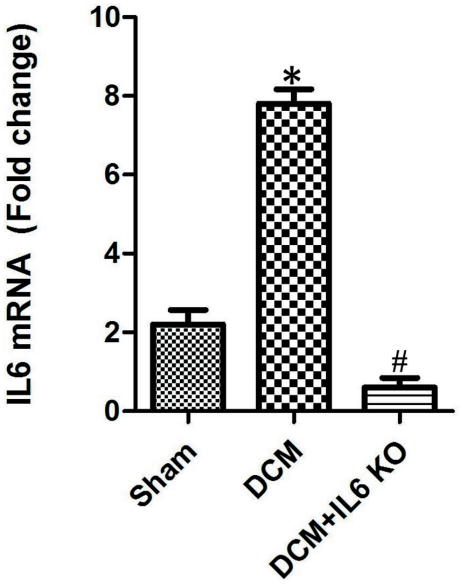

Figure 1. IL-6 expression in myocardial tissues in DCM mice Sham: Sham group, DCM: DCM group, +IL-6 KO: DCM+IL-6 KO group. *$p<0.05$ *vs.* Sham group, and #$p<0.05$ *vs.* DCM group, showing statistically significant differences.

Effects of IL-6 Knockout on Cardiac Morphology and Cross-Sectional Area of Myocardial Cells in DCM Mice

The HW/BW ratio in the three groups was detected. The results showed that the heart became significantly enlarged and the cross-sectional area of myocardial cells was significantly increased in HE staining in DCM group compared with those in Sham group ($p<0.05$). The pathological changes in the heart were significantly suppressed after IL-6 was inhibited (Figure 2).

Effect of IL-6 Knockout on Cardiac Function of Mice in Each Group

The results of echocardiography manifested that there was no statistically significant difference in BPM among the three groups, so the differences in EF (%) and FS (%) caused by BPM could be excluded. As shown in Figure 3, the ventricular cavity was enlarged and the heart wall became thinner in DCM group compared with those in Sham group, while the abnormal changes in the cardiac structure of DCM mice could be significantly inhibited after IL-6 knockout. Furthermore, FS (%) and EF (%) in each group were detected, and it was found that IL-6 knockout significantly raised FS (%) and EF (%) in DCM mice ($p<0.05$). The above results indicate that inhibiting IL-6 can improve the cardiac function of DCM mice.

Effect of IL-6 Knockout on Myocardial Fibrosis in Mice in Each Group

The myocardial fibrosis level in each group was evaluated using Masson staining and PSR staining. As shown in Figure 4, IL-6 knockout could remarkably inhibit the myocardial interstitial fibrosis in DCM mice. At the same time, the immunohistochemical staining was performed to detect the expressions of Collagen I and Collagen III in myocardial tissues in each group, and it was found that the expression levels of Collagen I and Collagen III in myocardial tissues of DCM mice significantly declined after the IL-6 expression was inhibited.

Terminal Deoxynucleotidyl Transferase-Mediated dUTP Nick End Labeling (TUNEL) Staining of Myocardial Tissues in Each Group

The number of apoptotic cells in myocardial tissues in each group was detected *via* TUNEL staining. As shown in Figure 5, the number of apoptotic cells in myocardial tissues was markedly increased in DCM group ($p<0.05$). After IL-6 knockout, the myocardial apoptosis level in

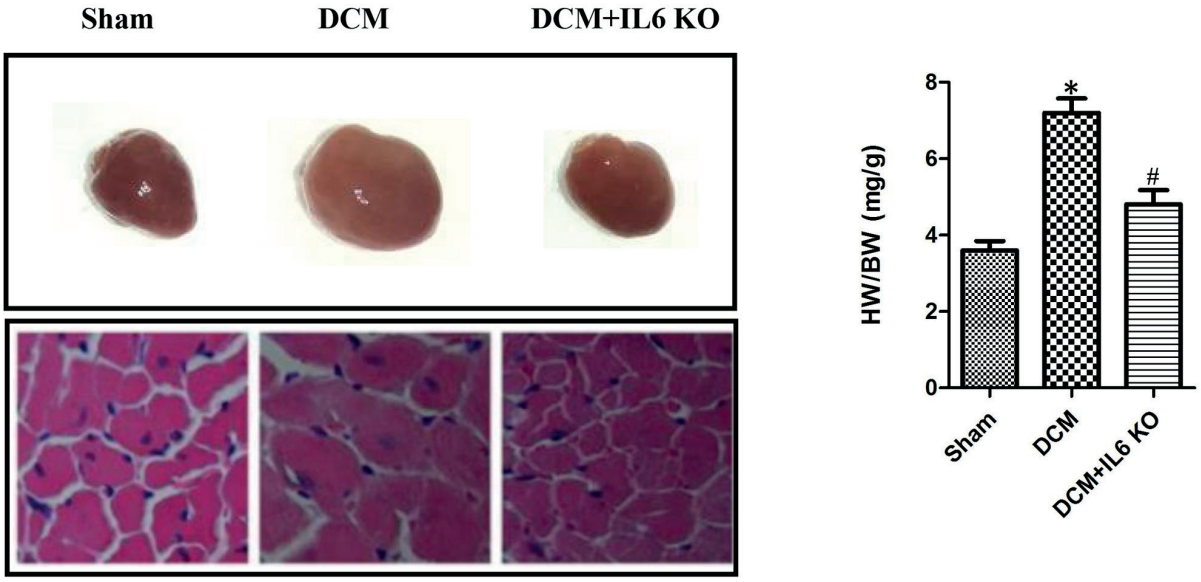

Figure 2. Effects of IL-6 knockout on cardiac morphology and cross-sectional area of myocardial cells in DCM mice (magnification: 400×). Sham: Sham group, DCM: DCM group, +IL-6 KO: DCM+IL-6 KO group. *$p<0.05$ *vs.* Sham group, and #$p<0.05$ *vs.* DCM group, displaying statistically significant differences.

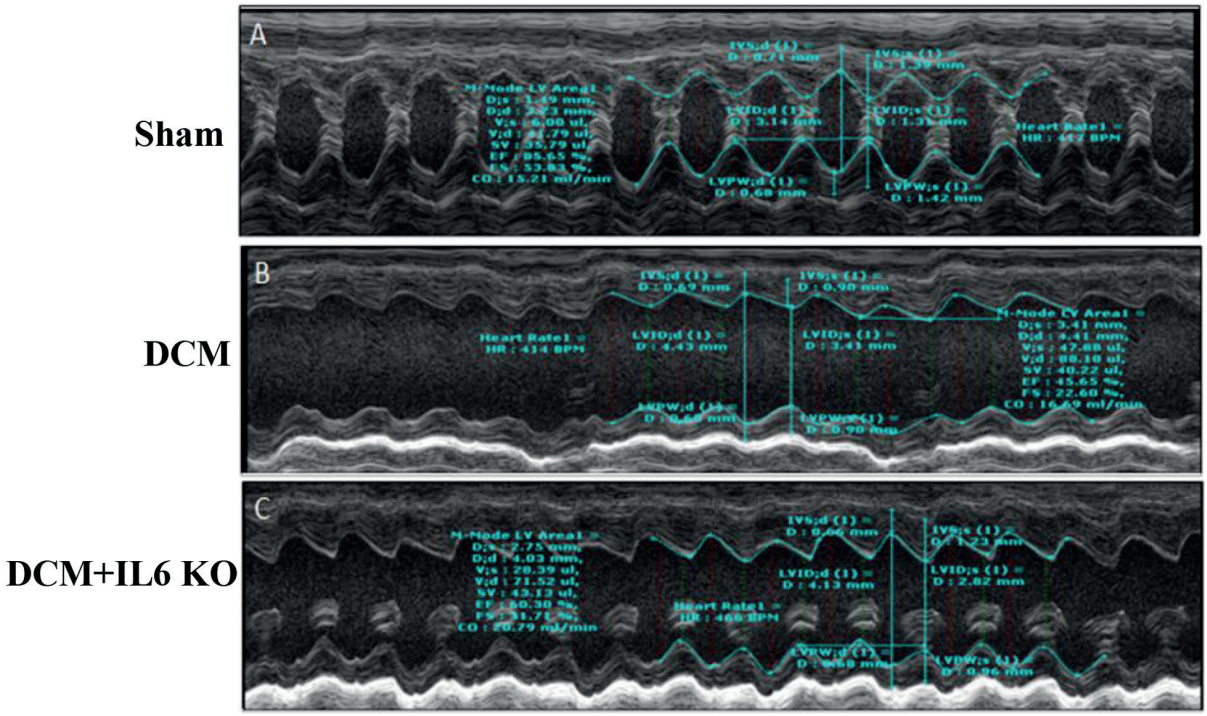

Figure 3. Effect of IL-6 knockout on cardiac function of DCM mice. Sham: Sham group, DCM: DCM group, +IL-6 KO: DCM+IL-6 KO group.

myocardial tissues of DCM mice significantly declined ($p<0.05$).

Expression of Apoptosis-Related Proteins in Myocardial Tissues in Each Group

Considering the important role of myocardial apoptosis in the occurrence and development of DCM, the expression levels of Bax and Bcl-2 in the heart in each group were detected ($p<0.05$). It was found that DCM+IL-6 KO group had a notably lower Bax/Bcl-2 ratio in myocardial tissues than DCM group ($p<0.05$) (Figure 6), indicating that the myocardial apoptosis level was lower in DCM+IL-6 KO group.

Effect of IL-6 Knockout on STAT3 Signaling Pathway

Finally, the expression levels of STAT3 signaling pathway-related proteins in myocardial tissues in each group were detected. The results showed that phosphorylated STAT3 (p-STAT3) was markedly activated in myocardial tissues in DCM group, while the phosphorylation of STAT3 was significantly inhibited after IL-6 knockout ($p<0.05$) (Figure 7).

Discussion

DCM contains multiple cardiac phenotypes and can be caused by a variety of myocardial damage. As one of the major causes of heart failure, DCM frequently occurs in young people, which is one of the most common indications for heart transplantation[10]. In fact, DCM is a non-specific phenotype, namely the final response of myocardial cells to a series of genetic and environmental damage[3]. The pathogenesis of DCM is complex, the widely-accepted mechanisms include genetic mutation, immune disorders, and stress (such as perinatal period) currently, and the interaction among a variety of genes or proteins lead to the occurrence and development of DCM[1]. At present, no satisfactory results have been achieved in the clinical treatment of DCM, and the prognosis of patients is extremely poor with a 5-year survival rate of lower than 50%[11,12]. Therefore, it is necessary to further explore the signal regulatory mechanism in the pathogenesis of DCM, and search for the key targets for DCM, so as to provide certain references for the clinical treatment and basic research on DCM.

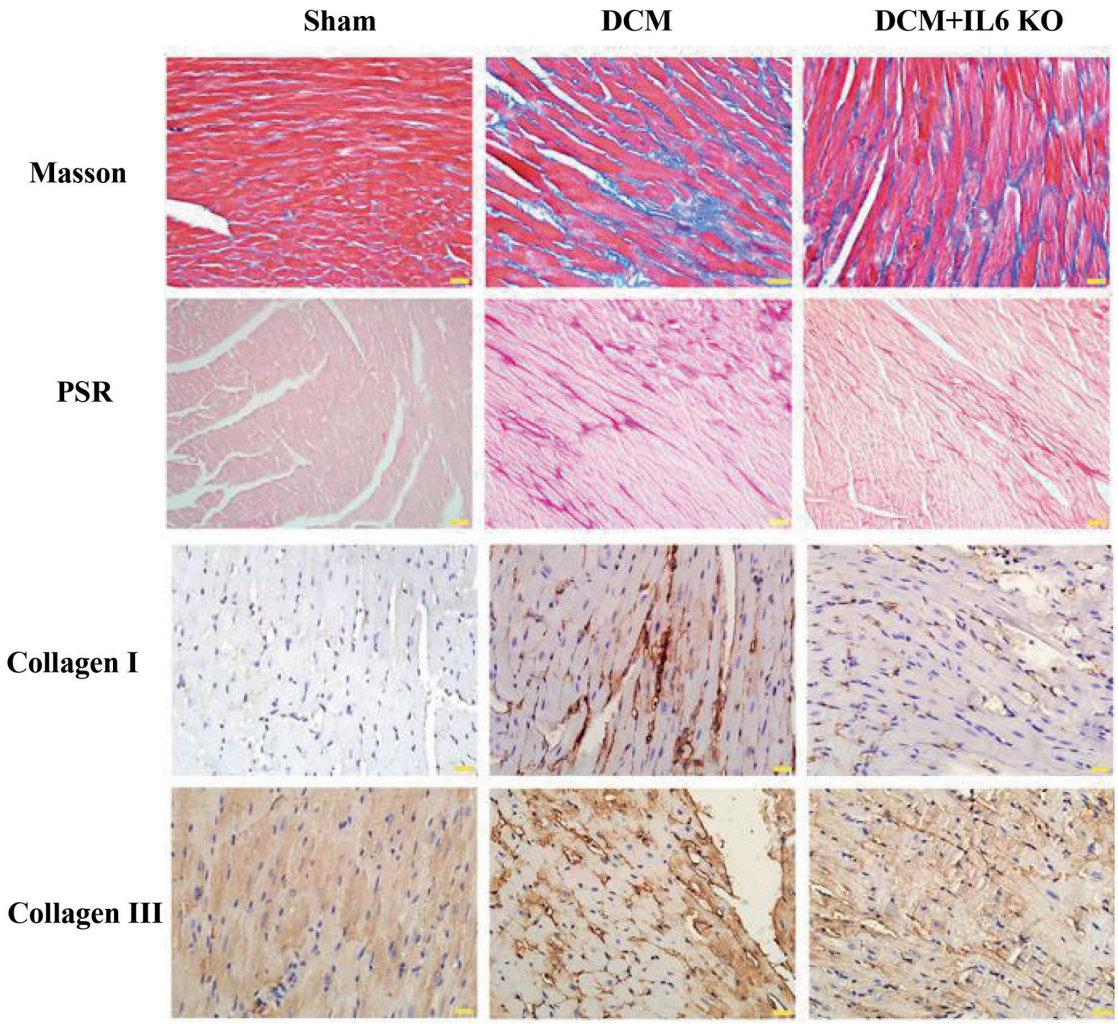

Figure 4. Effect of IL-6 knockout on myocardial fibrosis in DCM mice (magnification: 100×). Sham: Sham group, DCM: DCM group, +IL-6 KO: DCM+IL-6 KO group.

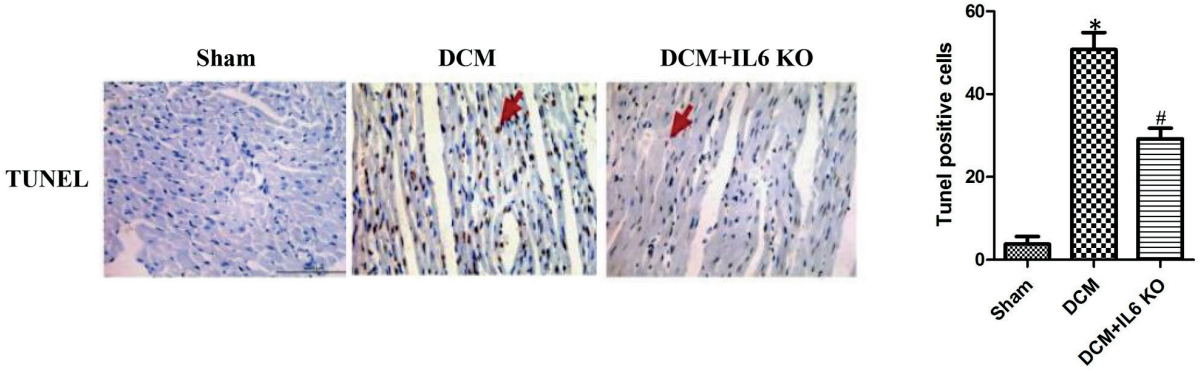

Figure 5. Effect of IL-6 knockout on myocardial apoptosis in DCM mice (magnification: 100×). Sham: Sham group, DCM: DCM group, +IL-6 KO: DCM+IL-6 KO group. *p<0.05 *vs.* Sham group, and #p<0.05 *vs.* DCM group, showing statistically significant differences.

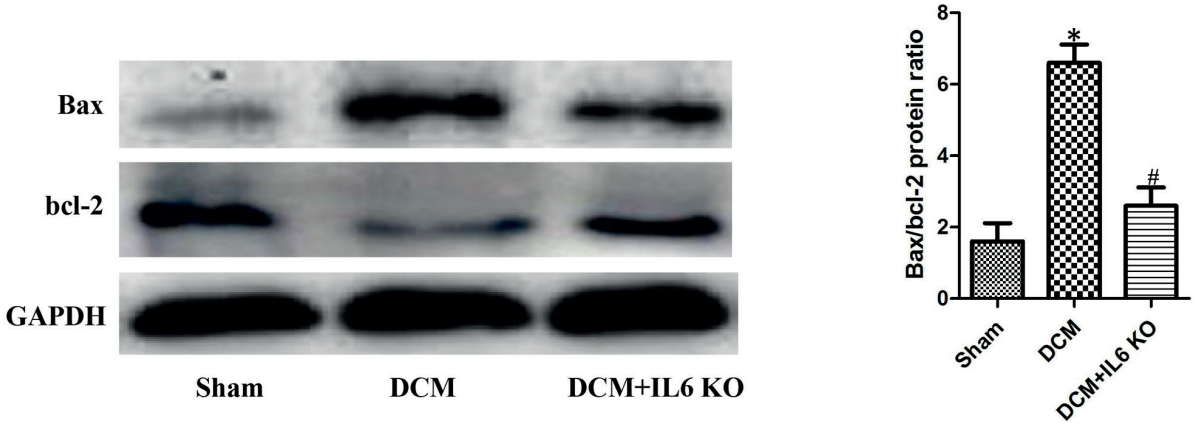

Figure 6. Effect of IL-6 knockout on expression of apoptosis-related proteins in DCM mice. Sham: Sham group, DCM: DCM group, +IL-6 KO: DCM+IL-6 KO group. *p<0.05 *vs.* Sham group, and #p<0.05 *vs.* DCM group, showing statistically significant differences.

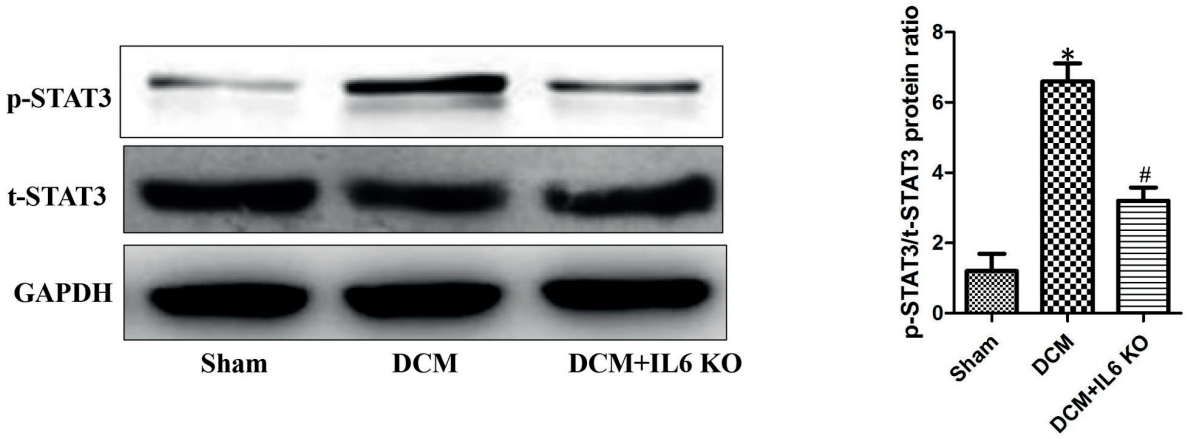

Figure 7. Effect of IL-6 knockout on expressions of STAT3 signaling pathway-related proteins in myocardial tissues in DCM mice. Sham: Sham group, DCM: DCM group, +IL-6 KO: DCM+IL-6 KO group. *p<0.05 *vs.* Sham group, and #p<0.05 *vs.* DCM group, exhibiting statistically significant differences.

There are seven members (STAT1-7) in the STAT family, and they are all expressed in myocardial tissues. In particular, STAT1 and STAT3 play the most evident role in cardiovascular diseases[13,14]. The STAT proteins have about 750-850 amino acids, the structural arrangement of their functional motif is similar, and the pairwise sequence homology is 20-50%[15]. The STAT proteins have dual effects: (1) they transmit the information from a variety of extracellular polypeptide signals through transmembrane receptors, and (2) they also provide a mechanism that can regulate gene transcription without the need of secondary messengers[16]. After the activation of the Janus kinase (JAK)/STAT pathway, cellular signals can be transmitted from the plasma membrane to the nucleus, which plays an important role in cardiovascular diseases. When the ligand binds to its isogenous cell surface receptors and induces partial conformational changes in the cytoplasm, the classical STAT signal activation will begin, thereby initiating the auto- or trans-phosphorylated activation of JAK protein[14]. JAKs are a family of four non-receptor tyrosine kinases (JAK1, JAK2, JAK3, and TYK2), which provide a docking site for STATs on a single tyrosine residue and selectively phosphorylate it. Evidence suggests that STAT3 is partially located in the mitochondria, and about 10% of cytoplasmic STAT3 is located in mitochondrial organelles. The deletion of STAT3 in myocardial cells in mice reduces the enzymatic activity of mitochondrial electron

transport chain complexes I and II by 50%, thus weakening the respiration of myocardial cells[17]. STAT3 also plays an important role in regulating the cardiac microenvironment. STAT3 is necessary for myocardial cells to secrete EPO to the surrounding environment, as well as for the expression of CCR2 ligand CCL2, both of which are indispensable for the differentiation of cardiac endothelial cells[18,19]. Moreover, the activation of STAT3 in cardiac fibroblasts can promote cell survival and proliferation, in addition to promoting the synthesis of extracellular matrix (ECM) components. It has been proved that IL-6, through activating STAT3, induces cardiac fibroblasts to produce collagen *in vitro*. The above results indicate that STAT3 plays a dual role in the heart[20]. In the present work, we found that STAT3 was significantly activated in the DCM model, and its expression was affected by IL-6. After IL-6 knockout, the cardiac function was significantly improved, and the myocardial remodeling, especially myocardial fibrosis, was significantly inhibited in DCM mice. Furthermore, IL-6 knockout suppressed the myocardial apoptosis level in DCM mice, and it also inhibited the expression of pro-apoptotic genes and promoted the expression of anti-apoptotic genes. Finally, IL-6 knockout inhibited the phosphorylation of STAT3 in heart tissues of DCM mice. However, there are still some limitations in the present study: 1) the cell experiments were not designed for verification, and 2) the effect of IL-6 overexpression on the occurrence and development of DCM was not proved through IL-6 injection.

Conclusions

We found for the first time that IL-6 knockout can improve the cardiac function and inhibit the cardiac remodeling and myocardial apoptosis in DCM mice, whose mechanism may be related to the regulation of IL-6 on the STAT3 signaling pathway.

Conflict of Interest

The Authors declare that they have no conflict of interest.

References

1) McNally EM, Mestroni L. Dilated cardiomyopathy: genetic determinants and mechanisms. Circ Res 2017; 121: 731-748.
2) Kankeu C, Clarke K, Passante E, Huber HJ. Doxorubicin-induced chronic dilated cardiomyopathy-the apoptosis hypothesis revisited. J Mol Med (Berl) 2017; 95: 239-248.
3) Halliday BP, Cleland J, Goldberger JJ, Prasad SK. Personalizing risk stratification for sudden death in dilated cardiomyopathy: the past, present, and future. Circulation 2017; 136: 215-231.
4) Yuan F, Qiu ZH, Wang XH, Sun YM, Wang J, Li RG, Liu H, Zhang M, Shi HY, Zhao L, Jiang WF, Liu X, Qiu XB, Qu XK, Yang YQ. MEF2C loss-of-function mutation associated with familial dilated cardiomyopathy. Clin Chem Lab Med 2018; 56: 502-511.
5) Le Dour C, Macquart C, Sera F, Homma S, Bonne G, Morrow JP, Worman HJ, Muchir A. Decreased WNT/beta-catenin signalling contributes to the pathogenesis of dilated cardiomyopathy caused by mutations in the lamin a/C gene. Hum Mol Genet 2017; 26: 333-343.
6) Fang T, Guo B, Xue L, Wang L. Atorvastatin prevents myocardial fibrosis in spontaneous hypertension via Interleukin-6 (IL-6)/signal transducer and activator of transcription 3 (STAT3)/endothelin-1 (ET-1) pathway. Med Sci Monit 2019; 25: 318-323.
7) Sales-Marques C, Cardoso CC, Alvarado-Arnez LE, Illaramendi X, Sales AM, Hacker MA, Barbosa M, Nery J, Pinheiro RO, Sarno EN, Pacheco AG, Moraes MO. Genetic polymorphisms of the IL6 and NOD2 genes are risk factors for inflammatory reactions in leprosy. PLoS Negl Trop Dis 2017; 11: e5754.
8) Stabile LP, Egloff AM, Gibson MK, Gooding WE, Ohr J, Zhou P, Rothenberger NJ, Wang L, Geiger JL, Flaherty JT, Grandis JR, Bauman JE. IL6 is associated with response to dasatinib and cetuximab: Phase II clinical trial with mechanistic correlatives in cetuximab-resistant head and neck cancer. Oral Oncol 2017; 69: 38-45.
9) Maass DL, White J, Horton JW. IL-1beta and IL-6 act synergistically with TNF-alpha to alter cardiac contractile function after burn trauma. Shock 2002; 18: 360-366.
10) Halliday BP, Gulati A, Ali A, Guha K, Newsome S, Arzanauskaite M, Vassiliou VS, Lota A, Izgi C, Tayal U, Khalique Z, Stirrat C, Auger D, Pareek N, Ismail TF, Rosen SD, Vazir A, Alpendurada F, Gregson J, Frenneaux MP, Cowie MR, Cleland J, Cook SA, Pennell DJ, Prasad SK. Association between midwall late gadolinium enhancement and sudden cardiac death in patients with dilated cardiomyopathy and mild and moderate left ventricular systolic dysfunction. Circulation 2017; 135: 2106-2115.
11) Nakamori S, Dohi K, Ishida M, Goto Y, Imanaka-Yoshida K, Omori T, Goto I, Kumagai N, Fujimoto N, Ichikawa Y, Kitagawa K, Yamada N, Sakuma H, Ito M. Native T1 mapping and extracellular volume mapping for the assessment of diffuse myocardial fibrosis in dilated cardiomyopathy. JACC Cardiovasc Imaging 2018; 11: 48-59.
12) Du G, Chen J, Wang Y, Cao T, Zhou L, Wang Y, Han X, Tang G. Differential expression of STAT-3 in subtypes of oral lichen planus: a preliminary study. Oral Surg Oral Med Oral Pathol Oral Radiol 2018; 125: 236-243.

13) Yu QN, Guo YB, Li X, Li CL, Tan WP, Fan XL, Qin ZL, Chen D, Wen WP, Zheng SG, Fu QL. ILC2 frequency and activity are inhibited by glucocorticoid treatment via STAT pathway in patients with asthma. Allergy 2018; 73: 1860-1870.

14) Jupatanakul N, Sim S, Anglero-Rodriguez YI, Souza-Neto J, Das S, Poti KE, Rossi SL, Bergren N, Vasilakis N, Dimopoulos G. Engineered Aedes aegypti JAK/STAT pathway-mediated immunity to dengue virus. PLoS Negl Trop Dis 2017; 11: e5187.

15) Villarino AV, Kanno Y, O'Shea JJ. Mechanisms and consequences of Jak-STAT signaling in the immune system. Nat Immunol 2017; 18: 374-384.

16) Banerjee S, Biehl A, Gadina M, Hasni S, Schwartz DM. JAK-STAT signaling as a target for inflammatory and autoimmune diseases: current and future prospects. Drugs 2017; 77: 521-546.

17) Fan Z, Gao Y, Huang Z, Xue F, Wu S, Yang J, Zhu L, Fu L. Protective effect of hydrogen-rich saline on pressure overload-induced cardiac hypertrophyin rats: possible role of JAK-STAT signaling. BMC Cardiovasc Disord 2018; 18: 32.

18) Jin H, Fujita T, Jin M, Kurotani R, Namekata I, Hamaguchi S, Hidaka Y, Cai W, Suita K, Ohnuki Y, Mototani Y, Shiozawa K, Prajapati R, Liang C, Umemura M, Yokoyama U, Sato M, Tanaka H, Okumura S, Ishikawa Y. Cardiac overexpression of Epac1 in transgenic mice rescues lipopolysaccharide-induced cardiac dysfunction and inhibits Jak-STAT pathway. J Mol Cell Cardiol 2017; 108: 170-180.

19) Chen Y, Surinkaew S, Naud P, Qi XY, Gillis MA, Shi YF, Tardif JC, Dobrev D, Nattel S. JAK-STAT signaling and the atrial fibrillation promoting fibrotic substrate. Cardiovasc Res 2017:

20) Sun XJ, Mao JR. Role of Janus kinase 2/signal transducer and activator of transcription 3 signaling pathway in cardioprotection of exercise preconditioning. Eur Rev Med Pharmacol Sci 2018; 22: 4975-4986.